

Computational evaluation of wind loads on buildings: a review

Agerneh K. Dagne¹ and Girma T. Bitsuamlak^{*2}

¹Laboratory for Wind Engineering Research, International Hurricane Research Center/Department of Civil and Environmental Engineering, Florida International University, Miami, Florida 33174, USA

²Associate Director WindEEE Research Institute, Department of Civil and Environmental Engineering, University of Western Ontario in London, Boundary Layer Wind Tunnel Laboratory Rm. 105, ON, Canada, N6A 5B9

(Received March 15, 2012, Revised July 12, 2012, Accepted October 6, 2012)

Abstract. This paper reviews the current state-of-the-art in the numerical evaluation of wind loads on buildings. Important aspects of numerical modeling including (i) turbulence modeling, (ii) inflow boundary conditions, (iii) ground surface roughness, (iv) near wall treatments, and (v) quantification of wind loads using the techniques of computational fluid dynamics (CFD) are summarized. Relative advantages of Large Eddy Simulation (LES) over Reynolds Averaged Navier-Stokes (RANS) and hybrid RANS-LES over LES are discussed based on physical realism and ease of application for wind load evaluation. Overall LES based simulations seem suitable for wind load evaluation. A need for computational wind load validations in comparison with experimental or field data is emphasized. A comparative study among numerical and experimental wind load evaluation on buildings demonstrated generally good agreements on the mean values, but more work is imperative for accurate peak design wind load evaluations. Particularly more research is needed on transient inlet boundaries and near wall modeling related issues.

Keywords: wind loads; building; computational fluid dynamics; turbulence; ABL; RANS; LES; hybrid LES-RANS; and validation

1. Introduction

Buildings, bridges, and all other civil engineering structures must be able to withstand external loads imposed by nature, such as wind, at least to the extent that the disastrous damage of natural force is reduced to the designed acceptable limit (Irwin 2008, 2009). Traditionally wind loads on buildings are obtained from building standards and codes. The majority of building codes and standards usually provide loads for along-wind direction of regular shape buildings under open and suburban exposure. Most often, building standards and codes utilize the quasi-steady and stripe theories approach where the gustiness of wind is customarily factored in by a random-vibration using the “gust factor approach” to predict the along-wind response (Davenport 1967, Simiu 1976). For example, the American Society of Civil Engineers (ASCE) 7-05 Standard contains provisions on wind loads for the design of Main Wind Force Resisting Systems (MWFRS), as well as Cladding and Components (C&C) of buildings with common shapes in open

*Corresponding author, Associate Professor, E-mail: gbitsuam@UWO.ca

and suburban terrain. Additionally, the National Building Code of Canada 2005 (NBCC 2005) provides acceleration calculations for the along-wind and across-wind directions. The Australian/New Zealand Standards (AS-NZ) (2002) code and the Architectural Institute of Japan (AIJ) recommendations (2400a) have made an exceptional attempt to provide the across-wind response using a cross-wind spectrum and expressions for both the across-wind and torsional root-mean-square acceleration. For cases not addressed by the building codes and standards, a physical testing in a boundary layer wind tunnel (BLWT) is referred. Although this option is economically viable for large projects such as the aerodynamics of tall buildings and long span bridges, performing building specific BLWT testing might not be cost-effective for most buildings such as low-rise residential buildings. Moreover, the variations in the wind flow and surrounding conditions that result from one project may not be extendable to a new project making generalizations more difficult. To address this gap at least for a preliminary wind load evaluation case, a computational model that can simulate the atmospheric boundary layer (ABL) flow and predict the parameters of interest can be an alternative approach. It is to be noted, however, computational approaches also have their own share of challenges and shortcomings yet to be resolved before their use for a final wind resistant design of buildings immersed in a turbulent ABL flows. At present, the cost of performing CFD is not lower than BLWT testing either. However, the computational cost is in a decreasing trend due to encouraging advances both in the hardware and software technology. This paper attempts to present a comprehensive review of the state-of-the-art of Computational Wind Engineering (CWE) as it relates to wind load evaluation on buildings. Recognizing significant progress made in the last decades, the paper will also pinpoint the area where the current practice of CFD needs further improvement, and attempts to discuss the direction of future CWE avenues based on the literature and authors' perspective, and draw some observatory conclusions relevant for practical applications of CWE.

Significant progress in CWE has been reported in literature. Ranging from: 2D to 3D flow field analysis; building to human scale; isolated buildings situated in open terrain to high-rise buildings located in urban city centers to complex environmental problems (Murakami 1998, Tamura *et al.* 2008, Jiang *et al.* 2006). Several published CWE findings dedicated to wind load evaluations supported with experimental validation have demonstrated encouraging results. Murakami (1997, 1998) have presented a historical review of turbulence modeling up to the late 1990s and pointed out the challenges that limited the practical applicability of CWE during that period. Some of the difficulties were: (a) high Reynolds number (Re); under this type of flow condition the accuracy of CWE is dependent on the grid resolution near the solid wall of the bluff body, (b) wind is complex, unsteady, and the 3D turbulent flow field is mainly characterized by impinging, separation, and vortex shedding. This requires 3D computation with an advanced turbulence model such as LES. However, the limitation in computing resources has hindered LES adoption in various CWE applications. Hence, it was common to carry out 2D RANS simulations during this period, (c) the presence of sharp edges at building corners make it very difficult to analyze the wind flow field by CFD, and (d) bluff body wake causes problems to inflow and outflow boundaries of LES and direct numerical simulation (DNS).

To overcome the aforementioned problems, several revisions have been made on RANS turbulence model closures mostly in an ad hoc manner. The revisions on RANS models, especially the modifications made on standard $k - \varepsilon$ models, succeeded in correcting the overestimation of kinetic energy production in the impinging region and reproduction of flow separation and reattachment around building roofs (Murakami 1997, Murakami and Mochida 1999). The LK model by Launder and Kato (1993) reduced the production of the kinetic energy at the windward

corner but had some mathematical inconsistency (Tsuchiya *et al.* 1997). Later Murakami *et al.* (1998) proposed the *MMK* model which provided significant improvements by removing the inconsistency of the *LK* model. A discussion on progress of CWE until the late 1990 was also provided by Stathopoulos (1999).

Some notable studies in the early 2000 include: non-linear RANS modeling for a full-scale low-rise building such as the Silsoe Cube (Wright and Easom 2003) where comparison of several $\kappa - \varepsilon$ family of turbulence models were provided in comparison with the field measurement data; computational prediction of flow-induced pressure fluctuations on Texas Tech University building (TTU) (Selvam 1999, Senthoooran *et al.* 2004). Gomes *et al.* (2005) simulated flow around L- and U- shape buildings by using the RNG $\kappa - \varepsilon$ turbulence model. Although good agreement between Gomez *et al.* (2005) and experimental results for upwind C_p values were observed, large discrepancies were found for C_p values of the wake regions mostly attributed to the use of isotropic turbulence model. More recently several CFD works have been reported on a bench mark tall building called the Commonwealth Advisory Aeronautical Research Council (CAARC) model building, which also commonly used as a benchmark for calibration/validation new BLWT facilities (Huang *et al.* 2007, Braun and Awruch 2009, Dagnew *et al.* 2009, 2010). Other works on tall buildings include: LES of a full-scale supper-tall building with Re greater than 10^8 (Huang and Li 2010); LES of flow and building wall pressure in a city center (Nuzu *et al.* 2008, Tamura 2010a); flow around a high-rise building using various turbulence models (Tominaga *et al.* 2008a); aerodynamic characteristics of a tall building inside a dense city district using LES (Tamura 2010b). The use of advanced turbulence modeling such as LES, and development of reliable and robust subgrid models and numerical algorithms which perform well in a wide range of flow parameters (Tamura *et al.* 2008) and prescriptions of transient inflow boundary (Sagaut *et al.* 2004, Tutar and Celik 2007, Xie and Castro 2008) reportedly have increased computational prediction accuracy.

Some countries have already established working groups to investigate the practical applicability of CWE (and for its potential inclusion in building codes and standards) and have developed recommendations and guidelines for efficient implementation and use for wind resistant design of actual buildings and for assessing pedestrian level winds. Within the framework of the Architectural Institute of Japan (AIJ) (Tominaga *et al.* 2008b) and the European cooperation in the field of scientific and technical research (COST 2007, Franke 2006). The AIJ provides methods for predicting wind loading on buildings by RANS and LES while COST Action 732 (COST 2007) outlined best practice guidelines for successful CFD simulations of wind flows in an urban environment using steady RANS equations. To this effect ASCE has also a task force which examines the potential use of CWE.

Wind loads and wind induced responses are affected in a complex way by several factors, such as oncoming wind characteristics (wind speed, turbulence intensity, integral length scales, etc.), topography and ground roughness, immediate surroundings, building shape, orientation, and dynamic structural properties (for flexible buildings). Hence, before getting to the wind load evaluation phase any CWE modeling should make an effort to incorporate these factors in the modeling process as realistically as possible to produce a usable outcome, just as is typically done in wind tunnel experiments. It is important to adopt/develop numerical models that realistically represent the complexity of the flow encountered while evaluating wind loads on buildings characterized as “bluff bodies” and submerged in a turbulent ABL flow. Because of this, challenges remain in numerically analyzing transient flow fields around bluff bodies. With this in

mind, major aspects of numerical wind evaluation focusing on turbulence modeling, computational domain (CD) and boundary conditions (BCs) will be discussed in the following sections. Existing numerical work on low- and high-rise buildings from literature and authors' own work will be compared among each other and with the experimental data. It is to be noted that the scope of this paper does not include non-conventional winds such as tornado and downburst.

2. Turbulence models

Choosing the right type of turbulence model is essential for accurate wind load evaluation. The selection of turbulence models is carried out by considering computational cost, level of modeling and resolution, and flow unsteadiness. The RANS and Reynolds Stress Model (RSM) have been widely used to simulate wind flow around bluff-bodies in the early stage of CWE. Encouraged by the increased computing power, the present trend in the modeling of complex wind/structure interactions are characterized by the desire to capture the unsteady turbulent motion, primarily to resolve the large-scale motions in time and space. Thus, Direct Numerical Simulation (DNS) and LES are better suited for such type of simulations. The multi-scale aspect and the concept of the kinetic energy cascade often describe the nature and complexity of turbulent flow. All the relevant active turbulence scales can be accurately represented by the DNS method without involving any modeling assumptions. In this method the total number of computational nodes may be scaled as (Re_L^3) , where Re_L denotes the Re number based on the spatial integral length. The presence of solid walls in the flow and the high magnitude of the relevant Re number ($10^5 - 10^8$, typical of tall buildings) substantially increase the computational cost and making DNS unpractical for wind load evaluations. Hereafter only LES and RANS or a combination of them will be discussed. Recently, the Hybrid method which includes a combination of RANS with LES (RANS-LES), very large-eddy simulation (VLES), and Partially Averaged Navier Stokes (PANS) equations is emerging as an alternative. Fig. 1 shows the classification of unsteady turbulence modeling approaches according to the level of modeling and readiness. The hybrid RANS-LES falls in the middle of the modeling and readiness level.

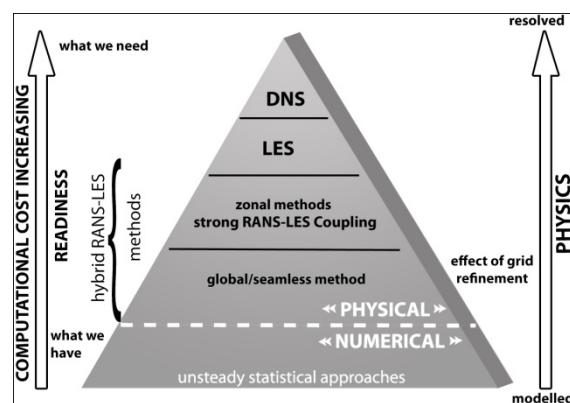


Fig. 1 Classification of unsteady approaches according to level of modeling and readiness (Sagaut *et al.* 2009)

2.1 The RANS models

Averaging of N-S equations in time and space can reduce the physical complexity of turbulent flow. Time averaging (steady RANS) or ensemble averaging (URANS) of N-S equations eliminate or partially eliminate the time dimension and produce mean flow characteristics. RANS based on linear eddy-viscosity models have been widely used in CWE applications. Various modifications and new modeling concepts have been developed, ranging from ad hoc remedies (empirical tuning of a set of constants), complex non-linear-eddy-viscosity approaches (NLEVM) to multi-equation and multi-scale second-moment closures, particularly for flows characterized by strong three-dimensional turbulence in which mean flow information is not sufficient enough to accurately predict unsteady flow behaviors (Hanjalić and Kenjereš 2008). However, oversimplified assumptions and the failure of the RANS modeling to capture some of the key phenomena (for example flow separations and reattachment for flow past a building) have limited its application for wind load evaluations. For wind-resistant design of an actual building, the use of RANS is limited to estimating time-averaged forces on the building, i.e., along-wind load (Tamura *et al.* 2008, AIJ 2004a, AIJ 2005). In the work of Hanjalić and Kenjereš (2008) some of the new advancements of RANS models aimed at robust application of realistic flows, in line with treatment of wall functions, have been discussed. Some of these new developments are identified as unsteady RANS, Multi-scale RANS, transient RANS, VLES and hybrid RANS/LES (Hanjalić, 2005). Even though, RANS is assumed to be the main strategy to drastically reduce computational cost, researchers are migrating from the traditional RANS modeling approach to advance turbulence modeling such as LES and Hybrid methods (Spalart 2009).

2.2 Large eddy simulation

As pointed out in the introduction, wind flows around buildings are complex, three dimensional, highly unsteady, and primarily characterized by high Re numbers and flow separations and reattachments “bluff bodies”. This result is significant in scale separation between the large-scale energy carrying structures and the small-scale dissipative eddies. Experience based knowledge showed that the calibration techniques in RANS, time and ensemble averaging, are very questionable for such flows. Decomposition of the resolved velocity field, prior to scale separation into “large-scale” and “small-scale” partitions, and the construction of a sub-grid stress tensor based on this decomposition is the foundation of the multi-scale approach of LES. LES offers a more comprehensive way of capturing unsteady flows. The dynamics of the large-scale structures are resolved, while the effect of small-scale turbulence is modeled using a sub-grid-scale (SGS) model. These basic strategies resolve most of the turbulent kinetic energy (κ) of the flow and model the dissipation (ϵ) which are assumed to have a weak effect (see Fig. 2) (Walters and Bushan 2005, Tucker and Lardeau 2009, Frölich *et al.* 2008).

LES modeling works well for high- Re number flow away from wall boundaries. However for an attached wall boundary where detailed near-wall treatment is required to capture the scale of motion responsible for turbulence production, a very large number of grid points and very small time steps are needed (Spalart 2009). For example, in the classical LES approach the wall units $\Delta x^+ \approx 50$, $\Delta y^+ \approx 1$, $\Delta z^+ \approx 15$ are used to capture the excited length and time-scales of turbulence near-wall regions (Sagaut and Deck 2009). However, for an attached wall boundary where detailed near-wall

treatment is required to capture the scale of motions responsible for turbulence production, high resolution both in space and time is needed (Spalart 2009) suggested that the level of resolution is attainable approximately in the year 2045. To alleviate the high computational cost of LES simulations, researchers suggested the hybridization of LES and RANS methods. While the free shear flow region with massive separation is treated by LES, the boundary layer is treated with RANS (Terracol *et al.* 2001). Recent studies by Grinstein and Drikakis (2007) showed that there is a growing interest in the implicit LES (ILES) method, particularly for external flows around buildings (Patnaik *et al.* 2007). In this method no subgrid scale (SGS) model is required for unresolved scales.

In the standard SGS model this is done by setting the Smagorinsky constant (C_s) to zero. The influence of the unresolved scales on the resolved scales is accounted for by the numerical dissipation of the discretization scheme of the convective terms in the momentum equations. The essential feature is that the numerical dissipation mimics sufficiently well the physical process of dissipation of the turbulent eddies.

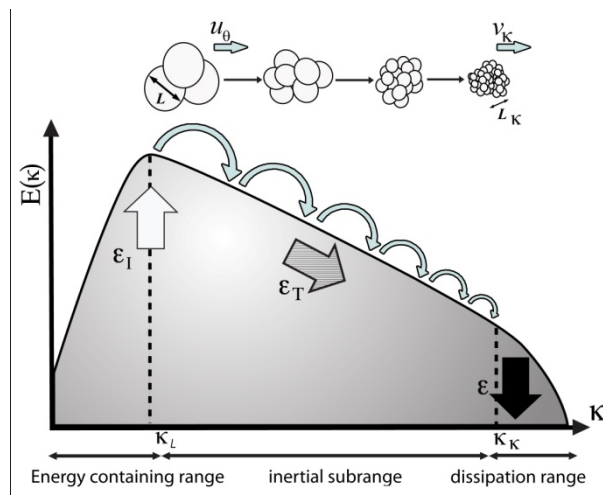


Fig. 2 Sketch of the energy cascade. In physical space, the large eddies are broken into smaller and smaller eddies (Sagaut *et al.* 2006)

2.2.1 SGS model in LES

In LES simulation, subgrid-scale stresses resulting from filtering operation of the N-S equations are unknown and requires modeling. Murakami (1997) reported the new trends in LES subgrid-scale modeling commonly applied for CWE applications. Since the introduction of the standard Smagorinsky SGS model (Deardorff, 1970), the dynamic Smagorinsky-Lilly SGS model based on Germano *et al.* (1996) and Lilly (1992) have become the standard of LES computation.

The Smagorinsky constant (C_s) is computed dynamically based on the resolved scales of motion.

Later Kim and Menon (1997) proposed the dynamic SGS kinetic energy model arguing that the subgrid-scale turbulence can be better modeled by accounting for the transport of the SGS turbulence kinetic energy. This approach was reported to perform better than an algebraic

expression based on the local equilibrium assumption given by the standard and dynamic Smagorinsky models (Huang *et al.* 2007).

2.3 Hybrid RANS/LES

Maintaining the balance between computational accuracy and computational cost is essential for turbulence modeling. The objection, i.e., because of high computational cost, of applying LES for the entire flow domain and the inadequacy of RANS modeling to capture the fluctuating components of lead to an alternative method, the Hybrid LES-RANS. This hybridization is assumed to efficiently blend the best features of RANS and LES and has recently become an attractive proposition for boundary layer flow simulations (Fröhlich and Dominic 2008). For pure LES simulation, the grid density increases with $Re^{1.8}$ in near-wall regions while in RANS grid clustering in the wall-normal direction is proportional to $\ln(Re)$ (Hanjalić *et al.* 2008). Hence, for flows where the attached boundary layer plays a dominant role in the flows, coupling of the models (LES and RANS) is arguably a better strategy to drastically reduce the computational cost of a stand-alone LES (Leschiziner 2009, Tucker and Lardeau 2009, Sagaut and Deck 2009, Hanjalić *et al.* 2008). Hybrid LES-RANS has been applied in various field of applications ranging from aeronautical (Forsythe *et al.* 2006), ground vehicles (Spalart and Squires 2004), scalar transport in urban environment (Lien *et al.* 2008) (Sreenivas *et al.* 2006) to buildings (Camarri *et al.* 2005, Wilson *et al.* 2006, Song and Park 2009).

The most common approaches in hybrid method are classified into two major classes, namely zonal (two-layer) and global (seamless) models. The zonal approaches are based on explicit splitting of computational domain into two distinct sub-domains and discontinuous treatment of RANS-LES interface. Coarse-grid LES is applied in the outer turbulent region, away from a solid wall, while a one-point RANS model is applied in the near-wall region. This is then coupled via appropriate boundary conditions at the RANS-LES interface (Sagaut *et al.* 2005, Hanjalić and Kenjereš 2008). In the seamless approach instead of switching models at the RANS-LES interface, a continuous treatment of flow variables are applied throughout the solution domain. The respective turbulence models will be activated by changing length scales. RANS, in the near wall flow regime, will be initiated using wall distance and LES in the outer turbulent region will be turned on using a representative grid size.

Despite the appealing feature of hybrid LES-RANS in reducing computational cost, there still remains some work to be done in both the “zonal” and “seamless” methods. For the zonal method, ensuring the proper matching of the conditions at the interface, location and definition of interface, and nature of matching condition are keys to it success. One way of attaining proper matching is by equaling the total stress or total viscosity. Since the RANS model contributes large portions of modeled quantities than LES, by either damping the eddy viscosity of RANS (using damping coefficient C_μ), decreasing RANS kinetic energy (increasing dissipation) the proper matching at the interface can be achieved (Hanjalić *et al.* 2004, Temmerman *et al.* 2005). Fig. 3(a) illustrates the zonal method with a different interface location. In addition, the stochastic backscatter approach by Piomelli *et al.* (2003); the addition of turbulent fluctuation by Davidson and Dahlstrom (2004), and the use of instantaneous C_μ by Hanjalić *et al.* (2004) are some of the proposed approaches for the reduction of non-physical features at the RANS-LES interface. In seamless method the continuity of the model (i.e., gradient continuity of eddy viscosity)

throughout the whole flow domain eliminates the need of a predefined interface. The “grid detecting” function controls the switching of the characteristic turbulence length scale L_{RANS} to L_{LES} (Fig. 3(b)). One of the most known hybrid approach under the seamless category is detached eddy simulation (DES) originally proposed by Spalart and Allmaras (1994), also called SA method. It applies a one-equation RANS modeling in the entire boundary layer while employing LES to separated regions. Later, Spalart *et al.* (1997) applied a modification to the original model by using a local equilibrium assumption, in which the production term is balanced by the destruction term. This approach turns the one equation SA model into an LES subgrid-scale model in regions where the grid resolution is high, and as RANS in the coarse mesh region. The gray area between the boundary layer and massive separation usually causes problems. This is usually handled using DES limiter by synthesizing to the grid spacing, i.e., replacing the wall distance ($\tilde{d} = \min(d, C_{DES} \cdot \Delta)$, where $\Delta = \max(\Delta x, \Delta y, \Delta z)$) by the filter width Δ will turn on LES (Travin *et al.* 2000, Breuer *et al.* 2003, Fröhlich and Terzi 2008). It is to be note that numerous studies have exhibited that the DES fails to serve its intended purpose when applied to flows with thick boundary layers and shallow separation regions (Breuer *et al.* 2003, Sagaut and Deck 2009).

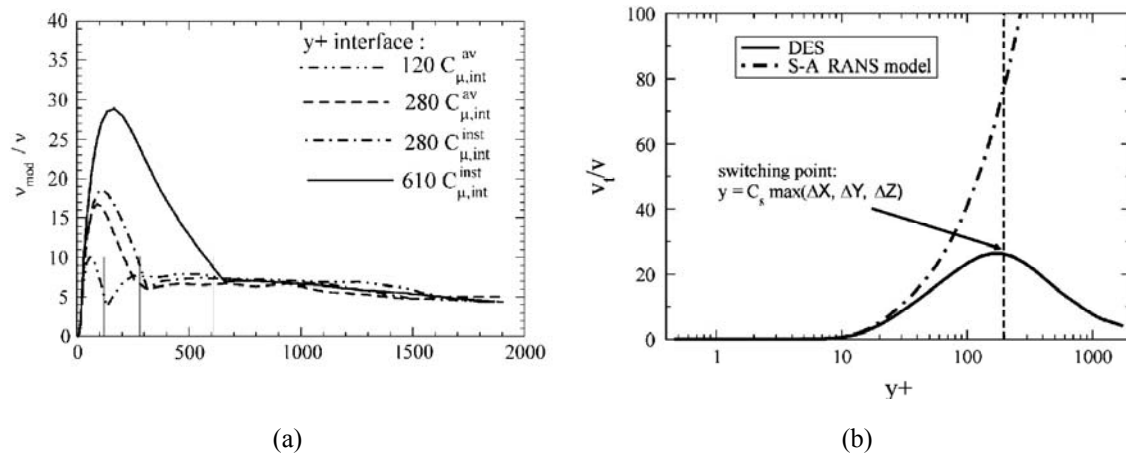


Fig. 3 Modeled eddy viscosity in hybrid RANS/LES methods. (a): zonal method with different interface locations and (b): seamless approach (Hanjalic and Kenjereš 2008)

Another challenge in the DES method is the mismatch of the mean velocity between the RANS and the LES region caused by the steep velocity gradient at the interface. In order to address this and other issues, recently a modified method called shielded and delayed detached eddy simulation (DDES) is proposed (Menter and Kuntz 2002, Spalart *et al.* 2006). In the new approach the DES limiter depends on the solution, i.e., the length scale, and preserve RANS mode by delaying the activation of LES, irrespective of the grid spacing. As an alternative approach, Girimaji *et al.* (2003) suggested the Partially Averaged Navier-Stokes (PANS) method based on the ratio of unresolved to total kinetic energy (k) and dissipation rate (ε). The ease of its implementation

into an existing RANS solver makes PANS a more attractive proposition for CWE application (Frohlich and Terzi 2008). Although hybrid RANS/LES is showing promising progress in terms of balancing computational cost and prediction accuracy more work needs to be done to address some of the challenges in merging RANS and LES. Based on the literature review and author's experience, LES is now a mature technique and is recommended for wind load evaluation application. In addition, the following numerical techniques contribute to the success of numerical wind evaluations: numerical generation of transient inflow turbulence (Kraichan 1970, Lund *et al.* 1998, Nozawa *et al.* 2002, 2003, Smirnov *et al.* 2001, Batten *et al.* 2004, Huang *et al.* 2010); development of advanced sub-grid scale turbulence modeling techniques capable of solving unsteady three-dimensional boundary separated flows; and numerical discretization with conservation of physical quantities for modeling complicated geometry. Because of these LES holds promise to becoming the future CWE modeling option of where turbulent flow is of pivotal importance (Tucker and Lardeau 2009, Sagaut and Deck 2009).

3. Computational domain and boundary conditions

The computational domain (CD) defines the region where the flow field is computed. The size of the CD should be large enough to accommodate all relevant flow features that will have potential impact on the characteristics of the flow field within the region of interest. In most cases, the stretch of the CD in the vertical, lateral and flow direction depends on the type of boundary conditions used. Franke (2006) and COST 2007 suggested that for a single building of height H , vertically the domain should extend $3H$ to $4H$ above the roof level if smaller blockage and up to $10H$ if larger blockage is anticipated. Based on these recommendations and from author's previous experience, the CD that extends $5H$ upwind will ensure the ABL to develop fully. If the inlet boundary is too far from the study building, the turbulence fluctuation will dissipate, this is true especially for wind load evaluation using LES, before it reaches to the study building. For RANS, the distance between the inlet and the incident plane should be long enough to preserve the mean velocity (U), the turbulent kinetic energy (k), and the turbulence dissipation rate (ε).

The outflow/or outlet boundary should be at far enough distance to allow the wake development. Hence $15H$ downstream of the target building is recommended. Laterally it can extend $5H$ from the sidewall surfaces. For LES additional requirements should be also taken into consideration when sizing the CD for example whether it is large enough to accommodate the formation of the largest energy containing flow structures (COST 2007).

Boundary conditions (BC) represent the effect of the surroundings that have been cut off by the CD and idealize the influence of the actual flow environment under consideration. BCs could dictate the solution inside the CD and have significant effects on the accuracy of the solution. At the inlet boundary, the mean wind velocity profile can be prescribed using either the power law or log-law profile. As a good practice a preliminary CFD simulation of an empty computational domain that accurately represents the ABL flow field should be performed by incorporating the measured flow data at the inlet boundary through numerical modeling (Blocken *et al.* 2007) (Fig. 4). For velocities, no-slip boundary is commonly used at solid walls (COST 2007). Although researchers have commented on the inadequacy of a smooth wall assumption, because of its relative ease of implementation, it is common to see simulations using this assumption (Tominaga *et al.* 2008a, Yoshie *et al.* 2007). For LES simulations, Murakami (1998) discussed the ineffectiveness of the no-slip boundary when applied to a bluff body with high Re and advised the

use of the Werner and Wengle (1991) wall function. One approach to address surface roughness issues is to evaluate the shear stress from the logarithmic relationship incorporated in the momentum equation between the wall and the first grid point (Mochida *et al.* 2002, Bitsuamlak *et al.* 2005). Blocken *et al.* (2007) who reviewed works of various researchers also emphasized on the effect of surface roughness in generating a homogeneous mean velocity profile and turbulent kinetic energy for RANS simulation. Symmetry boundary condition is usually employed at the top and lateral surfaces. Since details of the flow variables are not known prior to the simulation, an outflow boundary is usually applied at the outlet plane.

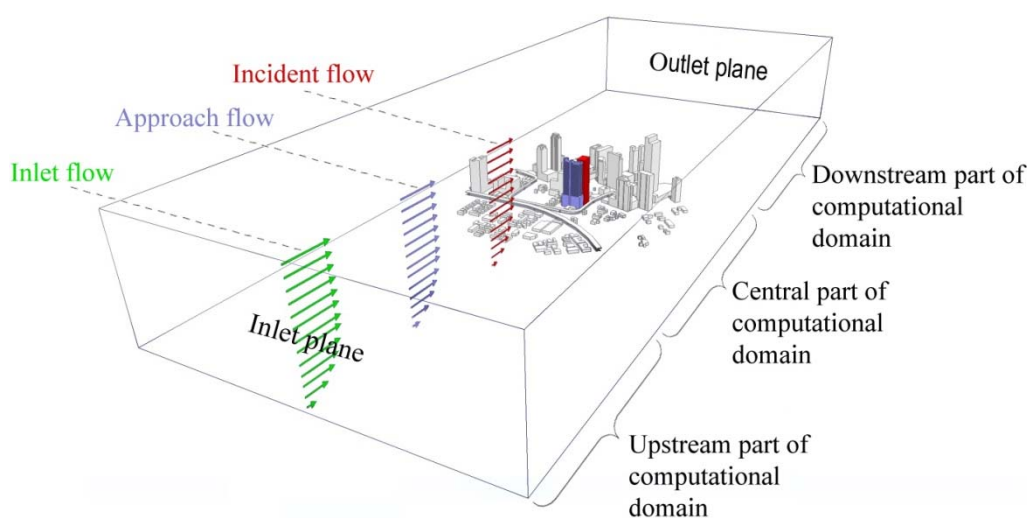


Fig. 4 Computational domain with building models for CFD simulation of ABL flow – definition of inlet flow, approach flow and incident flow and indication of different parts in the domain for roughness modeling (adopted and modified from Blocken *et al.* 2007)

4. Sources of wind inflow data for inlet boundary conditions

4.1 Target mean wind speed and turbulence intensity

Mean wind speed and turbulence intensity information at the study building location is obtained from meteorological data sources. Other common sources are building codes and standards. For example, ASCE 7-05 provides a 3sec gust basic design wind speed map for open terrain conditions at 33ft height, derived largely from meteorological stations at local airports. Field measurements and weather research forecasting (WRF) models (Skamarock *et al.* 2005) are also alternative sources. The ground surface roughness length is usually estimated by visually examining aerial photographs such as Google Earth photographs for each wind direction in comparisons with representative pictures given in building standards and codes. For inhomogeneous upwind terrain conditions and city centers this task is even more complicated. Some BLWT consulting firms, for example, use the Engineering Science Data Unit (ESDU) approach (ESDU 1993a,b). The mean wind speed values could be expressed in the form of

logarithmic (Eq. (1)) or power law (Eq. (2)) equations. Target turbulence statistics such as length-scale and turbulence intensity should be used as input as well. The turbulence intensity is defined as the ratio of the root mean square (σ_u) to the mean wind speed ($U(z)$), $I(z) = \sigma_u / U(z)$. Fig. 5(b) shows a typical streamwise velocity and turbulence intensity profiles for an open exposure. Figs. 5(c) and 5(d) show the typical streamwise velocity time history and power spectrum at the building height.

$$U(z) = \frac{1}{\kappa} u_* \ln\left(\frac{z}{z_0}\right) \tag{1}$$

$$U(z) = u(z_g) \left(\frac{z}{z_g}\right)^\alpha \tag{2}$$

where κ is the von Karman constant ($\kappa \approx 0.4$), u_* is the frictional velocity, z is the height above the ground surface, z_0 is the roughness length, α is an exponent dependent upon roughness of terrain, z_g is the gradient height, and $U(z)$ is the mean velocity at z distance from ground.

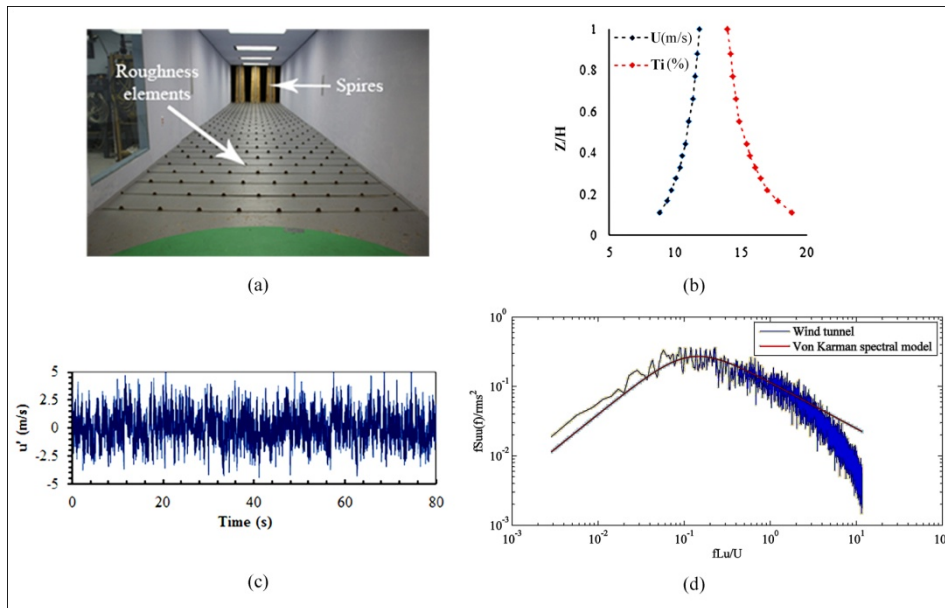


Fig. 5 (a) Trapezoidal planks & triangular floor roughness elements used for open exposure ABL simulation, (b) velocity profile (power law with $\alpha=0.14$) & turbulence intensity, (c) time history of streamwise velocity fluctuation and (d) Comparison of BLWT generated turbulence spectrum with von Karman spectrum model ($U_H = 12\text{m/s}$)

4.2 Numerical generation of transient inlet boundary for LES

For transient numerical modeling, in addition to the mean wind speed and turbulent intensity profiles, the transient wind characteristics are required in order to produce the peak or *rms* wind load. The success of LES and RANS/LES-based wind engineering applications, which require the transient time-history of fluctuating wind fields, heavily depends on the generation of accurate inflow turbulence at the inlet boundary. Inlet boundary conditions of LES simulation, of high *Re* turbulent flow, should possess an accurate representation of oncoming inflow turbulence, satisfying prescribed spatial and temporal correlations (Kondo *et al.* 1997, 2002, Tamura 2008). In high *Re* flows, the grid spacing is usually too coarse to resolve any large component of the turbulent spectrum due to computational power limitations. This especially occurs very near the inlet boundary, where few cells are allocated in order to reduce computational cost; the majority of the cells are allocated to resolve boundary layers, flow separation and attachment wakes and recirculating regions. The objective of the inlet boundary conditions is to supply turbulence integral length and time scales relevant to the grid Δx , Δy , Δz , and the computational time step Δt . Thus for transient simulation (such as URANS, LES, hybrid RAN-LES, and DNS), the inflow turbulence should be generated in accordance with the spatial and temporal resolution of the inlet boundary.

Most often the inflow turbulence due to the fluctuating velocity components are generated artificially using various numerical methods (Smirnov *et al.* 2001, Tutar and Celik 2007, Davidson 2007). The inflow turbulent generator could use flow statistics from existing BLWT database as well. There are several techniques to generate turbulence fluctuations. Huang *et al.* (2010) and Tabor and Baba-Ahmadi (2009) discussed various methods commonly used for generation of inflow turbulence at the inlet boundary of LES and hybrid RANS/LES simulation. These include recycling methods; precursor databases; and synthetic turbulence methods also briefly discussed here for completeness.

For unsteady numerical modeling, in addition to the mean wind speed and turbulent intensity profiles, the transient wind characteristics are required in order to produce the peak or *rms* wind load. The success of LES-based wind engineering applications, which require the transient time-history of fluctuating wind fields, heavily depends on the generation of accurate inflow turbulence at the inlet boundary. Inlet boundary conditions of LES simulations, of high *Re* turbulent flow, should possess an accurate representation of oncoming flow turbulence, satisfying prescribed spatial and temporal correlations (Kondo *et al.* 1997, 2002, Tamura 2008). In high *Re* flow simulations, computational grids are usually distributed systematically to manage the computational cost. As a result, in most cases, the grid spacing becomes too coarse to resolve any large component of the turbulent spectrum. This especially occurs very near the inlet boundary, where few cells are allocated in the upstream domain; whereas the majority of the cells are allocated in near-wall regions to resolve boundary layers, flow separation and attachment wakes and recirculating regions. However, the objective of the inlet boundary condition is to supply turbulence integral length and time scales relevant to the grid (Δx , Δy , Δz) and the computational time step (Δt). Thus, for transient simulation (such as URANS, LES, hybrid RAN-LES, and DNS) in addition to using high quality grid cells, the inflow turbulence should be generated in accordance with the spatial and temporal resolution of the inlet boundary. For example the spectrum depends on integral length scale $L(z)$, which is a function of height. One of

the following approaches can be adopted to generate transient inflow boundaries.

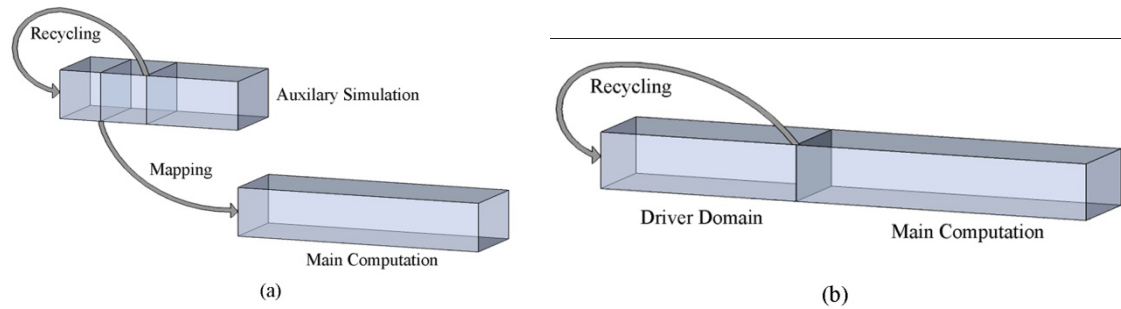


Fig. 6 Implementation of recycling method (Lund *et al.* 1998): (a) in which an auxiliary pre-computation is mined to produce the inlet velocities data and (b) computational domain is divided by driver and computation domain where data is passed on-the-fly to the main simulation

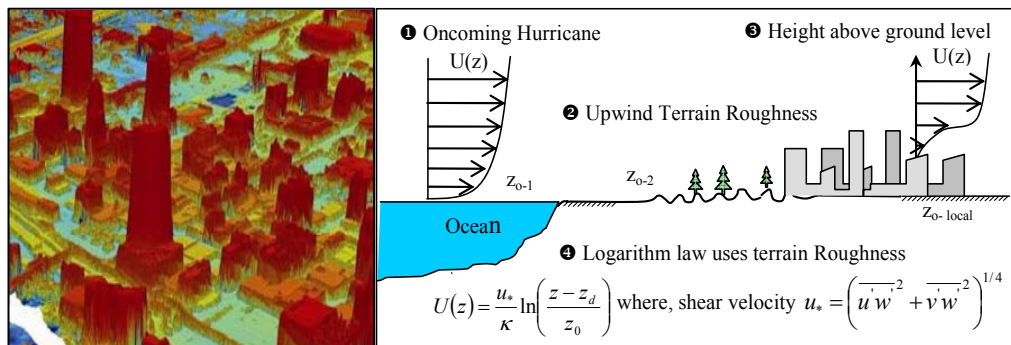


Fig. 7 (a) Surface roughness from LIDAR data and (b) the effect of surface roughness on the oncoming wind speed profiles (after Bitsuamlak *et al.* 2010)

4.2.1 Precursor simulation

Here, the simulation generates a library of turbulence databases that possess required flow characteristics such as temporal and spatial correlations. Once the desired turbulence flow characteristics are reached to a statistically stationary state, a time sequence of a 2D velocity field data will be extracted and stored. The inlet boundary of the main calculation uses these stored fluctuations by reading a plane of inflow data per time step (see Fig. 6(a)). This method is convenient when simulating inlet boundaries of small-scale high-resolution simulations from multi-scale CFD simulation that accounts the surface roughness of the upwind exposure directly (Bitsuamlak and Simiu 2010). Geographic Information System (GIS) applications such as LIDAR data, height of each structure and location-specific geographical information, that reflects realistically, the complexity of upwind roughness in urban areas and complex upwind terrain are very instrumental (Fig. 7). Although computationally expensive, the use of numerical simulations

on roughness geometry defined by LIDAR representing different exposure conditions on the upstream flow domain produced realistic inflow conditions at the inlet boundary (Abdi and Bitsuamlak 2010).

4.2.2 Recycling method

The recycling method is based on the Lund et al. (1998) proposal where the CD is divided into two domains. The domain upstream of the calculation domain, also called the “driver domain”, is used to generate spatially developing boundary layer flow. This is usually done by re-scaling the instantaneous velocity at the recycling plane and remapping the flow back to the inlet boundary. Once the simulation is performed for enough through-times and flow statistics are stable, a plane of data will be stored for later use by the main simulation. For the case where a combined simulation is carried out, the “calculation domain” will use the plane of data generated on the fly by the “driver domain” (see Fig. 6(b)). Nozawa and Tamura (2002) subsequently extend Lund’s method and employed it to a rough-wall boundary-layer flow. They applied this technique to simulate LES of flow around low-rise buildings immersed in a turbulent boundary layer flow and demonstrated that the mean and *rms* pressure coefficients were in good agreement with the BLWT data. Kataoka and Mizuno (2002) further simplified Lund’s method by assuming the growth of the inner boundary layer thickness is insignificant and assuming it is constant. Hence, instead of recycling the whole value of instantaneous velocity components only the fluctuating components are recycled. The velocity components at the inlet boundary are given as follow

$$u_{inlet}(y, z, t) = \langle u \rangle_{inlet}(z) + \phi(\theta) \times \{u(y, z, t) - \langle u \rangle(y, z)\}_{recy} \quad (3)$$

$$v_{inlet}(y, z, t) = \phi(\theta) \times \{v(y, z, t) - \langle v \rangle(y, z)\}_{recy} \quad (4)$$

$$w_{inlet}(y, z, t) = \phi(\theta) \times \{w(y, z, t) - \langle w \rangle(y, z)\}_{recy} \quad (5)$$

where the parenthesis $\langle \cdot \rangle$ denotes a time-averaged value in the span-wise direction and $\langle u \rangle_{inlet}$ is the prescribed mean velocity profile. The damping function $\phi(\theta)$ which prevents development of the turbulence in the free stream is given by

$$\phi(\theta) = \frac{1}{2} \left\{ 1 - \frac{\tanh[8.0(1-\theta)/(-0.4(\theta-0.3)+0.7)]}{\tanh(8.0)} \right\} \quad (6)$$

where $\theta = z/z_G$, z is the height, and z_G is the gradient height.

Inhomogeneous anisotropic inflow fluctuation fields can be generated by superimposing Lund’s recycling method with an artificially generated random perturbation for example by using the weighted amplitude wave superposition method (WAWS) (Swaddiwudhipong *et al.* 2007). The WAWS method is based on Shinozuka, (1985) where a fluctuation velocity field is generated from samples of a single random Gaussian process with zero mean and prescribed model energy spectral. For CWE application the wind energy spectrum in each direction is assumed to be

described by the von Karman model spectrum (Simiu and Scanlan 1996).

$$u'(t) = \sqrt{2} \sum_{k=1}^N \sqrt{S_u(f_k)} \Delta f \cos(2\pi f_k t + \varphi_k) \quad (7)$$

Where $S_u(f_k)$ is the one-sided von Karman spectral model of $u'(t)$, $f_k, k=1, \dots, N$ are the central frequencies of the interval Δf , and φ_k is the random phase angle uniformly distributed from 0 to 2π .

4.2.3 Synthesized turbulence

The synthesized turbulence fluctuation generation method proposed by Kraichnan (1970) uses an arbitrary energy spectrum as a function of a wave number to produce an isotropic perturbation. Inhomogeneous and anisotropic fluctuations have been investigated by various researchers (Smirnov *et al.* 2001, Batten *et al.* 2004, Billson *et al.* 2004), where the fluctuations were scaled in such a way that the time-averaged synthesized fluctuations match a prescribed Reynolds stress tensor. Smirnov *et al.* (2001) modified Kraichnan's method by incorporating turbulence length- and time -scales and succeeded in generating divergence-free fluctuations by synthesizing the velocity vector field from summation of the Fourier harmonic. A brief presentation of the random flow generation technique is given as follows

$$u_i(\tilde{x}, t) = \sqrt{\frac{2}{N}} \sum_{n=1}^N [p_i^n \cos(\tilde{k}_j^n \tilde{x}_j + \omega_n \tilde{t}) + q_i^n \sin(\tilde{k}_j^n \tilde{x}_j + \omega_n \tilde{t})] \quad (8)$$

where \tilde{x}_j, \tilde{t} are scaling parameters for the length- and time-scale of turbulence, k_i^n and ω_n are sample of wave number vectors and frequencies of the modeled turbulence spectrum, respectively. The Gaussian model spectrum employed in this method is expressed as

$$E(k) = 16(2/\pi)^{1/2} k^4 \exp(-2k^2) \quad (9)$$

The spectrum model is mainly designed to represent the large energy carrying structures and thus undermine the eddies within the inertial subrange (as shown in the shaded region of Fig. 8). However, turbulent ABL flows have demonstrated a cascade of energy between turbulent eddies. In such flow the inertial sub-range plays a vital role in transferring energy from large-energy containing range to small-scale eddies of dissipation range. The small-scale eddies in the dissipation range are in the same order of Kolmogorov scale (η) and the energy will eventually be converted to internal energy and dissipate. Considering the modeling principles of LES, i.e., resolving the flow up to the filtering (grid size) and modeling small-scales, the length-scale of inertial sub-range lies between the integral length scale and Kolmogorov scale and their contribution is very significant. For example the ANSYS Fluent 13 package has implemented this technique as a Spectral Synthesizer for generation of inflow turbulence at the inlet boundary of unsteady simulations. Hence, for computational wind engineering applications such as the wind effect on structures submerged in the ABL region, the inflow fluctuations should be representative

of a realistic turbulence spectrum such as the von Karman spectrum model (Lumley and Panofsky 1964, Li *et al.* 2007).

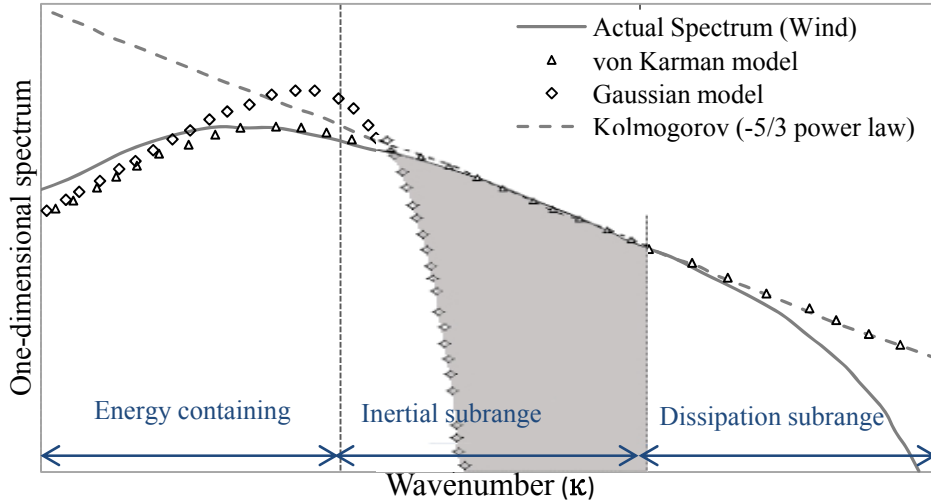


Fig. 8 Three turbulence subranges at high-Reynolds-numbers flow: Comparison of actual wind spectra with the von Karman and the Gaussian spectral model (after Hunag *et al.* 2010).

Later Huang *et al.* (2010) extended Kraichnan’s (1970) synthesizing technique to generate inhomogeneous inflow turbulence. The method, which is called the discretizing and synthesizing random flow generation (DSRFG) has the flexibility to prescribing any arbitrary 3D spectrum for the amplitude of the fluctuation, for example the von Karman spectral. The synthesized velocity field is presented below for discussion purposes and the detailed formulation and derivation can be found in the original paper

$$u(x, t) = \sum_{m=k_0}^{K_{mq}} \sum_{n=1}^N [p^{m,n} \cos(\tilde{k}^{m,n} \tilde{x} + \omega_{m,n} t) + q^{m,n} \sin(\tilde{k}^{m,n} \tilde{x} + \omega_{m,n} t)] \tag{10}$$

where $p^{m,n}$ and $q^{m,n}$ are the vector form of the fluctuation amplitude. For inhomogeneous and anisotropic turbulence the distribution of $k^{m,n}$ is done by remapping the surface of the sphere after the components of $P^{m,n}$ and $q^{m,n}$ are aligned with the energy spectrum.

In addition to the flexibility of prescribing any arbitrary 3D spectrum, the DSRFG method uses the length scale ($L_s = \sqrt{L_u^2 + L_v^2 + L_w^2}$) as a scaling factor and this resulted in the generation of spatially correlated flow fields with the relevant length scales. However, the method is M times expensive compared to the method proposed by Simirnov *et al.* (2001), where M is the number of discretization points.

Castro *et al.* (2011) pointed out some of the limitations on the DSRFG technique and suggested some modifications for the inhomogeneous and anisotropic field of the DSRFG method. In the DSRFG method the representation of the kinetic energy using diverging series and the quality of the generated flow field is heavily dependent on the number of discretization point M . The other is regarding the temporal correlation of the flow field generated by the DSRFG method. To address these issues the study proposed some modifications to the equations based on the shape of the energy spectrum. The formulation for the modified DSRFG also called MDSRFG method is presented as follow

$$u(x, t) = \sum_{m=1_0}^M \sum_{n=1}^N [p^{m,n} \cos(\tilde{k}^{m,n} \tilde{x} + \omega_{m,n} \frac{t}{\tau_0}) + q^{m,n} \sin(\tilde{k}^{m,n} \tilde{x} + \omega_{m,n} \frac{t}{\tau_0})] \quad (11)$$

$$p_i^{m,n} = \text{sign}(r_i^{m,n}) \sqrt{\frac{4c_i}{N} E_i(k_m) \Delta k_m \frac{(r_i^{m,n})^2}{1 + (r_i^{m,n})^2}} \quad (12)$$

$$q_i^{m,n} = \text{sign}(r_i^{m,n}) \sqrt{\frac{4c_i}{N} E_i(k_m) \Delta k_m \frac{1}{1 + (r_i^{m,n})^2}} \quad (13)$$

where τ_0 is time scaling parameter and c_i is a function that depends on the shape of the energy spectrum. The comparative studies on the inhomogeneous velocity fluctuation generated by the two methods are shown in Table 1. As it can be seen, in Table 1, although both the proposed methods, resulted *rms* value comparable to the target value, calculated as $TI * U_{avg}$, the MDSRFG method showed considerable improvement. Both methods with aligning and remapping techniques produced anisotropic flow field with strong spatial correlations, while MDSRFG showed better temporal correlation of the turbulence field.

Table 1 Comparison of the *rms* values of simulated velocity fluctuations (After Huang *et al.* 2010 and Castro *et al.* 2011)

Inflow turbulence generation method	Distribution method of $p_i^{m,n}$, $q_i^{m,n}$, and $k^{m,n}$	σ_u	σ_v	σ_w
DSRFG	Scaling & transformation	0.9968	2.4400	2.9956
DSRFG	Aligning & remapping	0.9500	1.9987	3.0800
MDSRFG	Aligning & remapping	1.0527	2.1850	3.1123
Target		1.1200	2.2400	3.3600

5. Need for CWE validation with experimental data

CWE applications are at a fairly young stage, it would be prudent to evaluate their prediction

accuracy through comparison with experimental laboratory as well as field measurements data. As described in Fig. 9, both full-scale and model-scale experiments could be used for validating CFD results of low- and high-rise buildings. In general, it is worthwhile to stress that comparing numerical simulations with experimental data should be carried out with full knowledge of basic facts such as wind flow field, the surrounding conditions, and exposure type. Steady and fluctuating wind forces (along- and across-wind) computed from a time history of pressures is very sensitive to data averaging length (Obsaju 1992). This is also true when applying LES for such evaluations, hence averaging time comparable with experimental data should be taken. Hence, the level of validation of these simulations should involve well sampled statistical analysis (Sagaut and Deck 2009). Table 2 summarized grades of various levels of validation.

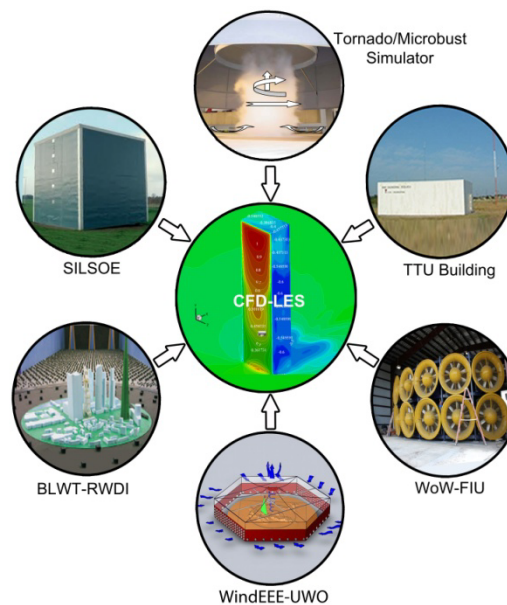


Fig. 9 Validation of CFD with model-scale and full-scale experiments, and field measurement. Note: Tornado simulator is from Iowa State University. TTU refers to Texas Tech University, FIU refers to Florida International University, UWO University of Western Ontario. RWDI refers to Rowan Williams Davis and Irwin Inc

6. Computational evaluation of wind load on buildings

6.1 Illustration of wind pressure loads on surface mounted cube

For testing and validating the accuracy of computational evaluations of wind pressures, the majority of numerical studies refer to the basic cube shape exposed to wind perpendicular to its face (Stathopoulos 2002, 2003). This is because the cube has a simple geometry with important complex features of a real building flow and abundant full-scale and experimental results available

in literature. Fig. 10 shows numerical and experimental studies of the surface mounted cube, Silsoe 6m cube, by several researchers. Wright and Easom (2003) compared the mean pressure coefficient on the surface of the Silsoe cube using standard $k-\epsilon$, RNG $k-\epsilon$ models (Yakhot *et al.* 1992) derived from the renormalization group of analysis of Navier-Stokes equations and MMK $k-\epsilon$ (Tsuchiya *et al.* 1997), which intends to improve the prediction of turbulent kinetic energy and eddy viscosity for a bluff body field, and DSM (Differential Stress Model) of Launder *et al.* (1975), which is a more complex anisotropic turbulence model. The prediction by RNG $k-\epsilon$, especially in the windward face where the standard $k-\epsilon$ model over-estimates the suction pressure, is in better agreement with the BLWT data. The revised $k-\epsilon$ models have improved the prediction accuracy on the separation region. However such adjustments are of an ad hoc nature and added improvements are only for some particular cases. Lim *et al.* (2009) C_p values obtained through LES simulation showed better agreement with the experimental data.

Table 2 Levels of validation of simulation techniques (Sagant and Deck 2009)

Grade	Level of validation
1	Forces (Lift, drag and moment)
2	Mean aerodynamic field (velocity profiles)
3	Second order statistics (<i>rms</i> quantities)
4	One-point spectral analysis (power spectral densities)
5	Two-point spectral analysis (correlation, coherence and phase spectra)
6	High-order and time-frequency analysis (time-frequency)

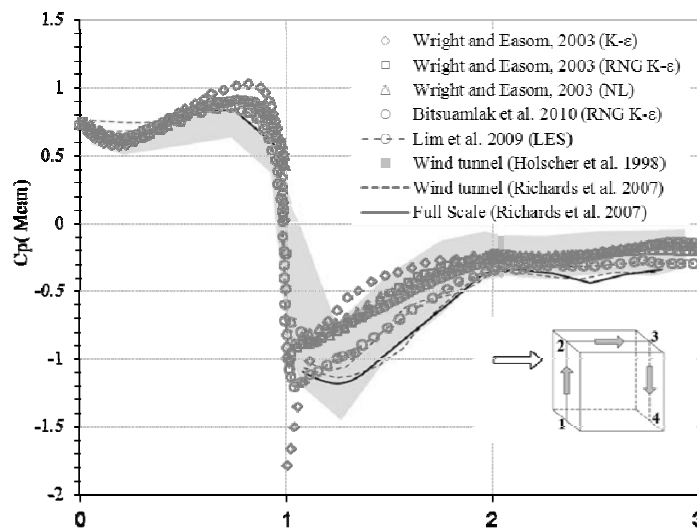


Fig. 10 Surface mounted cube: Comparison of mean wind pressure coefficients between wind tunnel experiments and numerical simulation by using several turbulence models (after Bitusamlak *et al.* 2010)

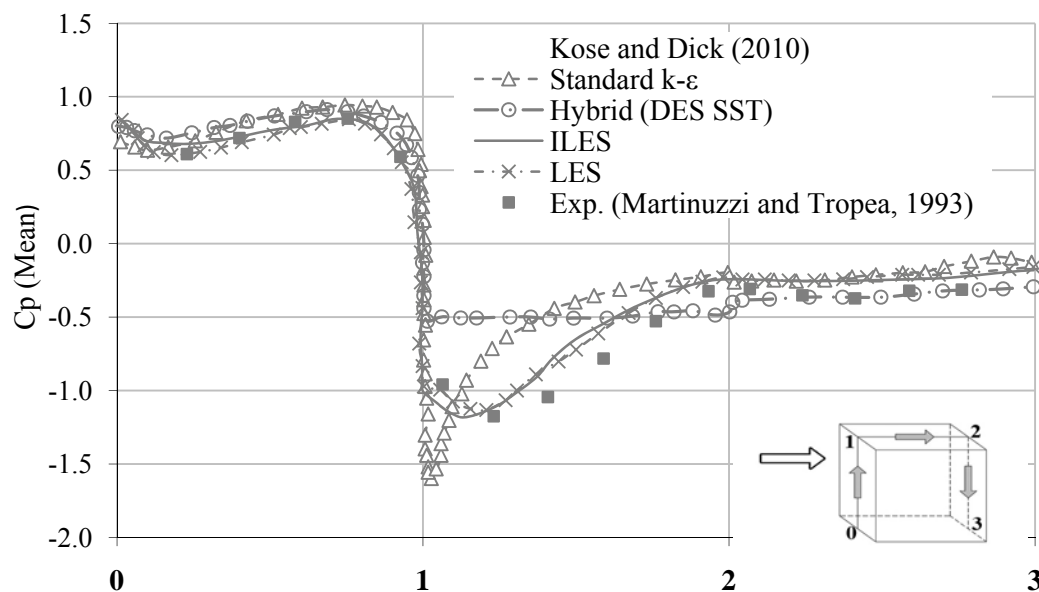


Fig. 11 Cubical building in ABL flow. Comparison of pressure coefficient profiles on the vertical section using several turbulence models (after Köse and Dick 2010)

Köse and Dick (2010) investigated the performance of RANS, hybrid RANS/LES, and implicit LES (ILES) turbulence models on coarse meshes. For the cases with coarse meshes, the study showed no significant differences between the results of the RANS and hybrid (DED SST) simulations, as shown in Fig. 11. In the case of the hybrid model, the poor prediction of the mean C_p at the front and side faces is attributed to the fact that the LES model in the outer region failed to behave as a pure LES. This is attributed to the coarseness of the grid used in the simulation. Considering the coarseness of the meshes used in the simulations, both the LES and ILES were reported to give better results. Fig. 12 shows CFD and experimentally obtained pressure coefficients at 45° wind angle of attack (Wright and Easom 2003). As expected the standard $k-\varepsilon$ appears to over predict the mean C_p , although the error seems to be reduced as compared to the prediction for the cube with the normal wind angle of attack, because of the reduced flow impingement.

6.2 Illustration of wind pressure loads on low-rise buildings

Several numerical studies have been reported for wind load evaluation of low-rise buildings. Tsuchiya *et al.* (1997) and Nozawa and Tamura (2002) predicted the mean pressure coefficients of short buildings with a size of $H: H: 0.5 H$. Fig. 13 shows the distribution of time-averaged pressure coefficients on the mid vertical plane of a low-rise building. Because of the impinging flow, the approaching flow did not separate from the leading edge of the roof, the standard $k-\varepsilon$ overestimates the C_p value on the frontal face. On the other hand, the approaching flows

simulated with the modified $k-\varepsilon$ models $\kappa-\varepsilon-\varphi$ (Kawamoto *et al.* 1998), and the *MMK* model (Tsuchiya *et al.* 1997) were separated from the leading edge of the roof and they resulted an improved prediction of the mean C_p at the windward face that were in closer agreement with the experiment data carried by Kondo (1997). Another noticeable observation is that, in all the $k-\varepsilon$ models the absence of velocity fluctuation due to vortex shedding effect, produced in smaller production of kinetic energy behind the building. While the LES simulation by Nozawa and Tamura (2002) well predicted the pressure coefficients on the surfaces of the building. However, the same study reported that the discrepancy in the inlet velocity profile caused the LES to overestimate *rms* coefficients on the roof.

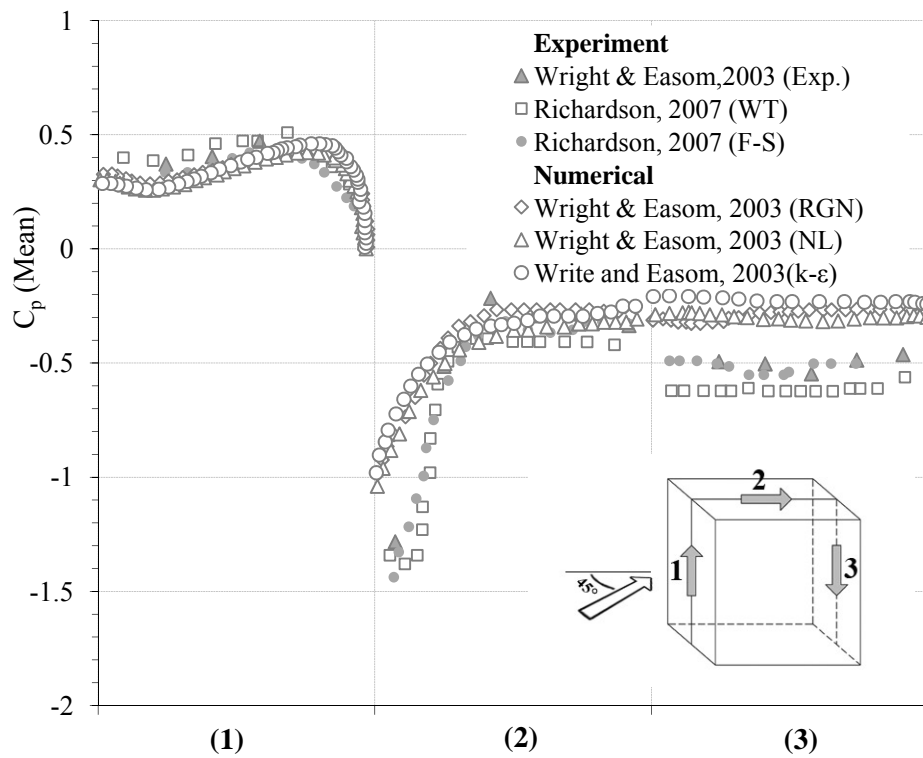


Fig. 12 Silsoe 6m cube: Comparison of mean pressure coefficient between full scale measurements, wind tunnel and numerical simulations- cube skewed at 45°

The TTU building is considered to be one of the extensively studied standard short buildings for wind loads. Senthoooran *et al.* (2004) evaluates the wind-induced pressure fluctuation of TTU using Kato and Launder's (1993) modified $k-\varepsilon$ turbulence model. The stochastic technique is used to generate the inflow turbulence fluctuation. The revised *MMK* model (Launder and Kato 1993), which eliminates the excessive production of kinetic energy around the impinging region performed better and the results are in a good agreement with the experimental data and field results (Fig. 14).

Recently, Köse and Dick (2011) performed an implicit LES (ILES) and LES simulations to

investigate the influence of inflow conditions on the quality of the mean pressure distribution on the same building. Fig. 15 compares the LES and ILES prediction along the centerline of a vertical plane of the TTU. Improvements on the mean C_p value have been observed after adjusting the inflow turbulence by reducing the kinetic energy. In both studies (Selvam 1997, Köse and Dick 2011) there was a considerable discrepancy between the numerical and the BLWT prediction, particularly the overproduction of the mean C_p at the windward face and roof surfaces. The overproduction is mainly caused by strong deformation of the oncoming flow velocity profile in the incident region.

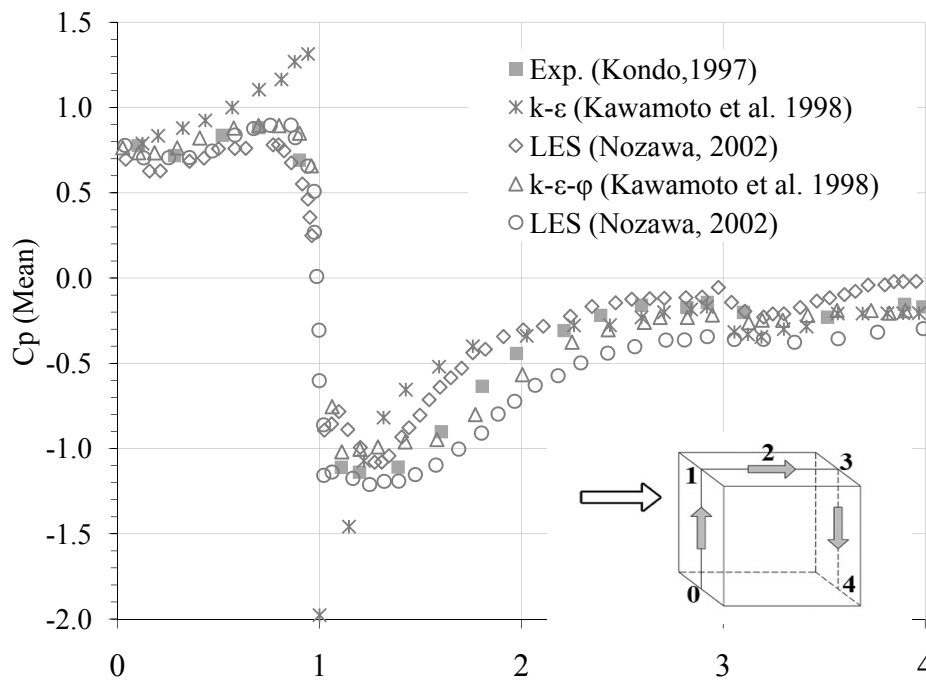


Fig. 13 Low-rise building: Comparison of mean wind pressure coefficients experiment and numerical (after Nozawa and Tamura 2002)

This shows how the wind pressure load distribution is sensitive to the incoming turbulence.

There is also an effort towards using the Partially Averaged Navier-Stokes (PANS) turbulence modeling for wind effect evaluation which is regarded as an alternative to the hybrid RANS/LES. The PANS modeling aims to capture/or resolve the energy containing structures at a reasonable computational cost, by using coarse computational meshes. The method uses the Boussinesq approximation technique for modeling the unresolved-scales (Abdol-Hamid and Girimaji 2005). Song and Park (2009) carried out a two-stage PANS simulation to evaluate the wind- pressure load on a square cylinder. Fig. 16 shows their PANS simulation, for various grid resolution cases, fairly predicted the mean C_p of the windward face, while it slightly over-predicted the pressure distributions on the sidewalls. The case with fine grids reproduced the velocity in the wake and recirculation region very well and resulted in an accurate prediction of the mean C_p on the leeward face and the mean drag coefficient by the high resolution simulation. The PANS method seems

heading in the right direction in addressing some of the grid dependence issues related to hybrid RANS/LES turbulence modeling. Although C_p comparison with the hybrid RANS/LES and LES would have provide more insight on the cost effectiveness and prediction accuracy of PANS.

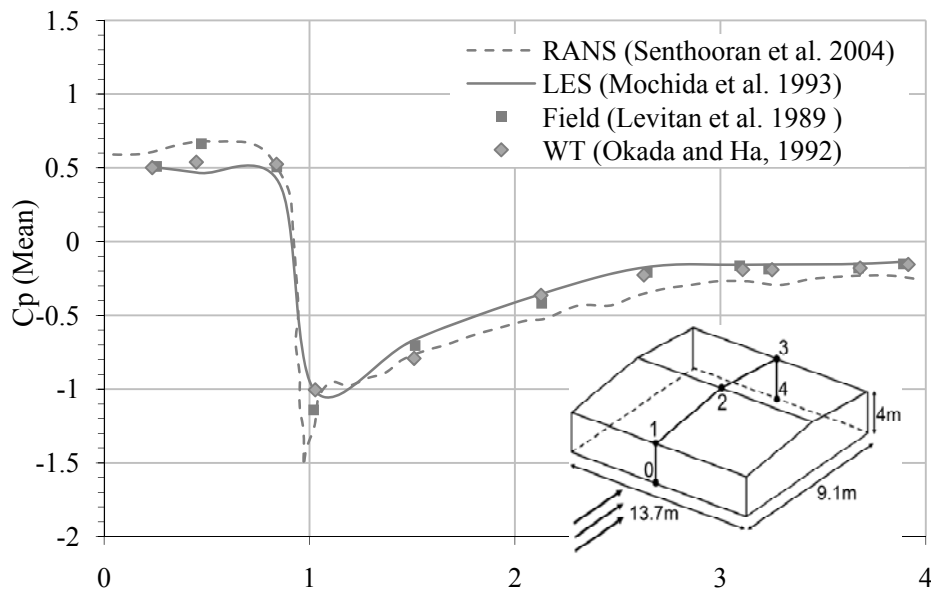


Fig. 14 The TTU building: Comparison between mean pressure coefficients for straight wind computational and WT and field measurements (after Senthoooran et al., 2004)

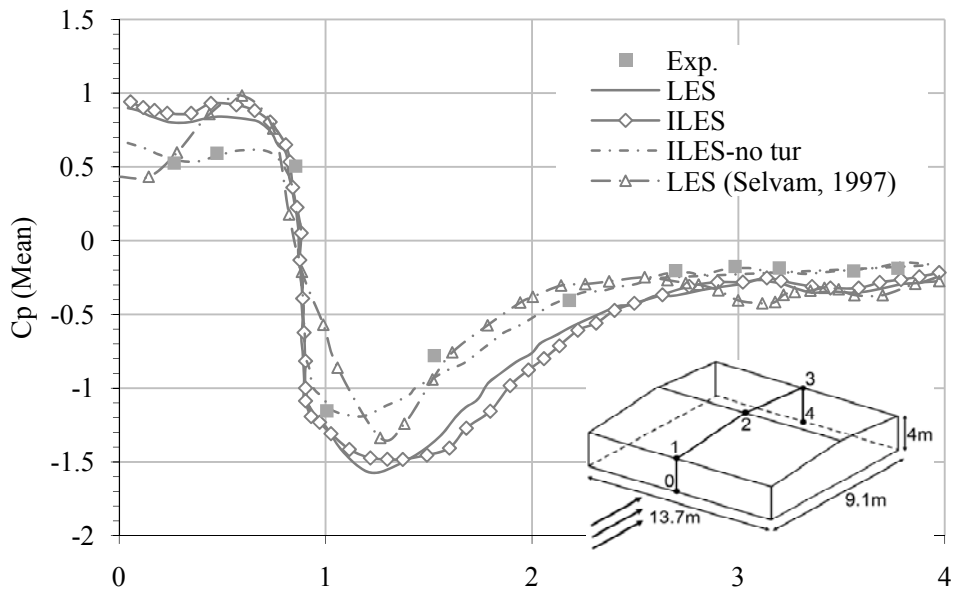


Fig. 15 The TTU building in ABL flow condition: Comparison of pressure coefficient profiles on the vertical section between wind tunnel experiments and numerical simulations (after Köse and Dick 2011)

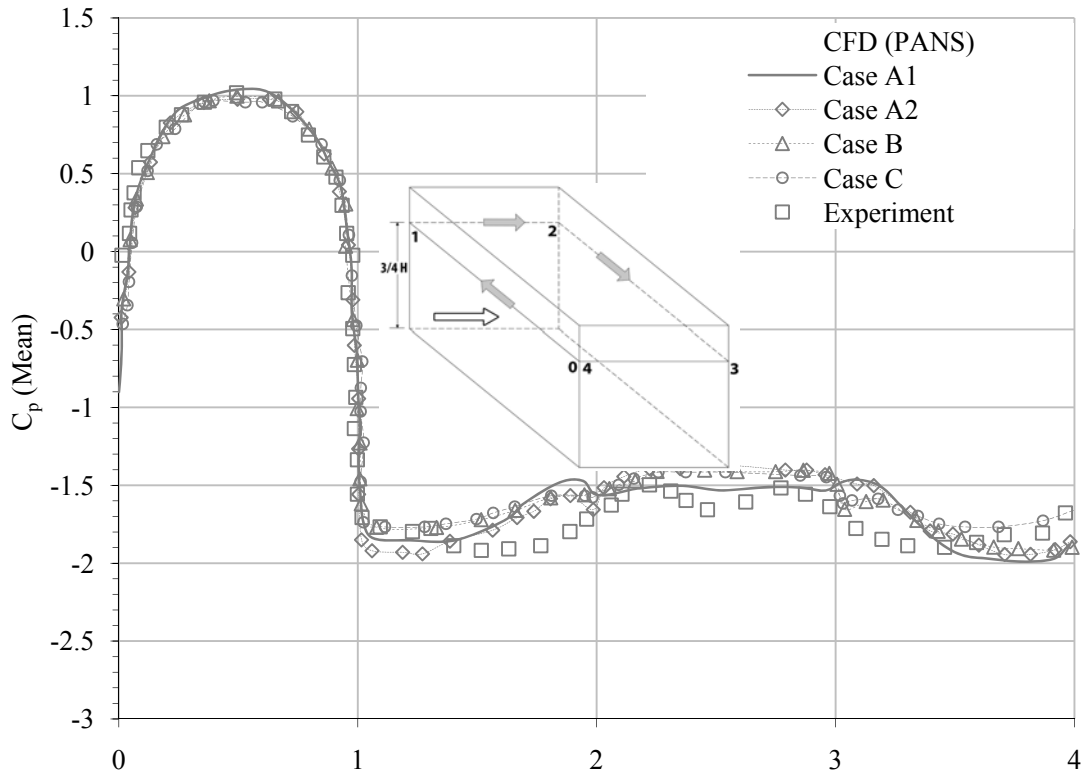


Fig. 16 Distribution of averaged pressure coefficient along the surface of the square cylinder (after Song and Park 2009). Where Case A1 and Case A2 have the same number of grids (204×122) in the vertical and stream-wise direction but the spans-wise grids of Case A1 is about two times of Case A2 (54 cells); Case B is with grid resolution of $187 \times 114 \times 40$; Case C is with grid resolution ($174 \times 108 \times 27$).

Overall the CFD results showed reasonable agreement with the measured BLWT and field data for time-averaged wind loads on low-rise buildings. However, more work is needed regarding the peak-wind load estimation using the some of the models such as LES. Numerical research should also look into how well the peak-loads compare with the experimental data in addition to the mean and *rms* values. As this will give strong ground for CWE application for design wind load evaluation.

6.3 Wind load estimation on high-rise buildings

The Commonwealth Advisory Aeronautical Research Council (CAARC) building model (Melbourne 1980) is used by several wind engineering experimental laboratories for calibration and validation purposes to study external aerodynamic loads of tall buildings. The CWE community is also using the same model to assess the performance of numerical wind load evaluation techniques for tall buildings. As part of this review study, the authors carried out a limited investigation for various inflow turbulence generation techniques for LES. Fig. 17 presents

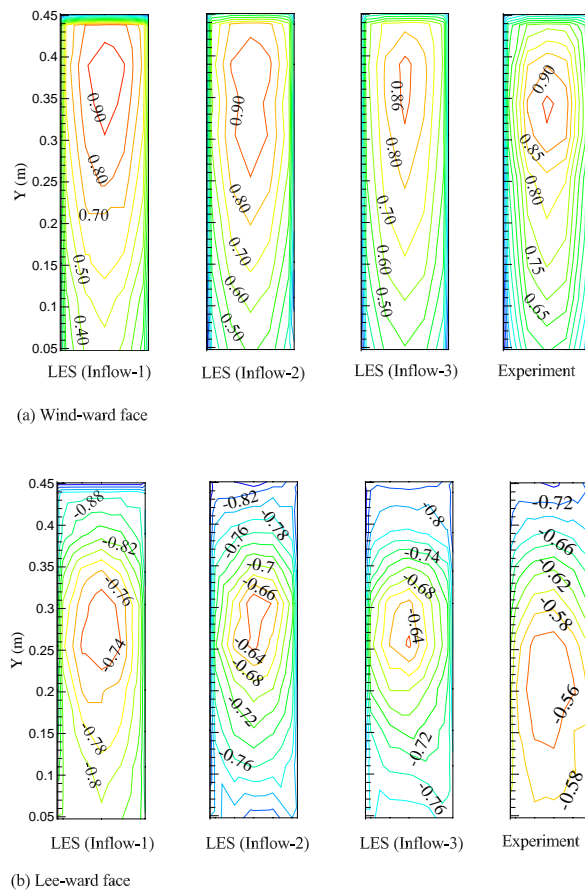


Fig. 17 Comparison between the mean pressure coefficients of CAARC in a simulated ABL flow using LES with various inflow turbulence models and BLWT experiment. Where Inflow-1 is the Spectral synthesizer method (Smirnov *et al.* 2001); Inflow-2 is the Recycling method (Lund *et al.* 1998); and Inflow-3 is based on the Synthesized turbulence method

the LES and wind tunnel data for the mean pressure coefficient acting on the wind- and lee-ward faces of the CAARC building model, produced by using the various numerical methods in Sec. 2.1.3.1). The BLWT test was carried out at RWDI Inc. The pressure coefficient distributions agree well with each other even from a quantitative point of view. On the wind-ward face, the LES mean C_p contours estimated by the three inlet boundaries (Inlet 1:Smirnov *et al.* (2001), Inflow 2: Lund *et al.* (1998); Inflow 3: following synthesizing method) showed good a agreement with the BLWT data. The LES predictions of the mean C_p for the lee-ward face

showed marginal discrepancy with the BLWT, compared to the better agreement observed for wind-ward face. Among, the three inflow conditions, Inflow-3 was marginally performing better than the Inflows-1 and -2 predictions. The distributions of fluctuating pressure coefficients presented in Fig. 18. The *rms* produced by the Inflow-3 on the wind-ward face, a place where the inflow fluctuation effect could be seen more apparently (compared to other faces which potentially experience more fluctuation due to flow separation) was in better agreement with the BLWT's *rms*. On the lee-ward face, the numerical result slightly deviated from the BLWT data. Although superimposing random fluctuations on a mean velocity profile (for example Inflow-1) is a simple way of generating inflow turbulence, the turbulence has weak spatial correlation and tends to decay rapidly (Kempf *et al.* 2005). The authors further investigated the effect of inflow turbulences on the dynamic wind load evaluation of a standard tall building using LES. It has been found that the fluctuating wind loads are very sensitive to perturbation imposed at the inlet boundary. Random inflow turbulence generated using the synthetic inflow generation technique showed a good spatial correlation of the fluctuating velocity component and the resulted predications were reasonably comparable with the BLWT data, especially the across-wind force spectra (Fig. 19). The along-wind force spectra also showed promising results, however better results could have been obtained if a longer averaging time was taken for the pressure time-history analysis of the LES simulation. For this study only two seconds (flow time) of data was recorded, because of computational resource limitation, and this greatly contributed to the discrepancy of the drag force compared to the BLWT data. Moreover, inhomogeneous turbulence with the von Karman spectrum better represents a realistic wind flow field and will significantly improve the prediction accuracy of LES. The authors are working at the moment on LES of a tall building under urban settings using the synthesized techniques of a random flow generator (such as DSRFG) as inlet boundary.

The comparison between the mean pressure coefficients of several computational (LES and RANS) and experimental studies of the CAARC building model extracted at $2/3$ of H (H is the height of CAARC building model) is shown in Fig. 20. On the wind-ward face the RANS based on the RNG $K - \epsilon$ model over-predicted, as expected, the mean C_p while the LES showed a better agreement with the BLWT data. Considerable discrepancy has been observed at the side face, where the flow separated because of the sharp corner. Similar studies (Huang *et al.* 2007, Braun and Awruch 2009) showed a good C_p prediction at the wind-ward face but a slight deviation in the side and lee-ward faces from the BLWT measurements have been observed. This discrepancy is due to the random inflow turbulence generated using the Gaussian spectrum model which under-estimated the eddies in the inertial subrange (as discussed in Sec. 4.4.3) and the assumption of the no-slip wall boundary condition used in the simulation. Dagnev *et al.* (2009) investigated the effect of the grid resolution for LES under turbulent flow. The case (LES1) with a high resolution mesh ($1 < y^+ < 5$) in the near-wall region resulted in a better prediction, especially in the windward face, with the BLWT data than the case (LES2) with Werner and Wengle (1991) wall function applied in the near-wall region. Hence it is a good practice to resolve the flow in the region of interest, such as the wall boundary and upwind domain.

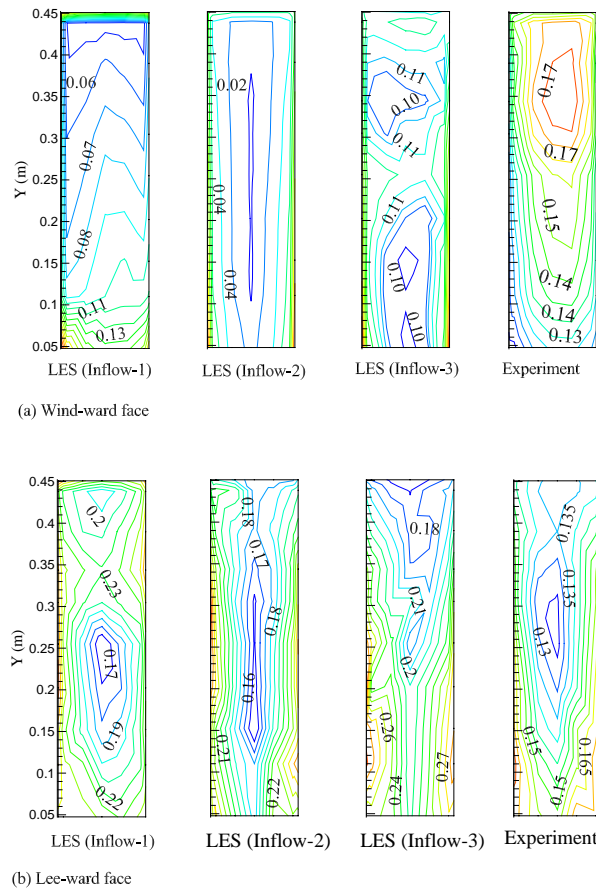


Fig. 18 Distribution of fluctuating pressure coefficient (rms) over the frontal and lee-ward faces of CAARC in a simulated ABL flow filed: Comparison between LES with various inflow turbulence models and BLWT experiment Where Inflow-1 is the Spectral synthesizer method (Smirnov *et al.* 2001); Inflow-2 is the Recycling method (Lund *et al.* 1998); and Inflow-3 is the Synthesized turbulence method

Nozawa and Tamura (2003) predicted the time-averaged pressure coefficients on a high-rise building (1:1:4) using an LES simulation (see Fig. 21(a)). Inflow turbulence was generated at the inlet boundary using a modified recycling method. This improved the numerical prediction of the mean pressure coefficient on the frontal surface of the high-rise building and the results are in good agreement with the BLWT data done by Ohtake (2002) and Kawai (1982). Fig. 21(b) shows the rms of pressure coefficients of the same study. There is a discrepancy in the rms coefficients on the roof of the high-rise building, this deviation was caused by a variation in the mean velocity profile. Tamura *et al.* (2008) presented the AIJ guidelines to the numerical prediction of wind loads on a building. The wind load on low-rise (1:1:0.5) buildings predicted by CFD was compared with those obtained from experiments and AIJ recommendations.

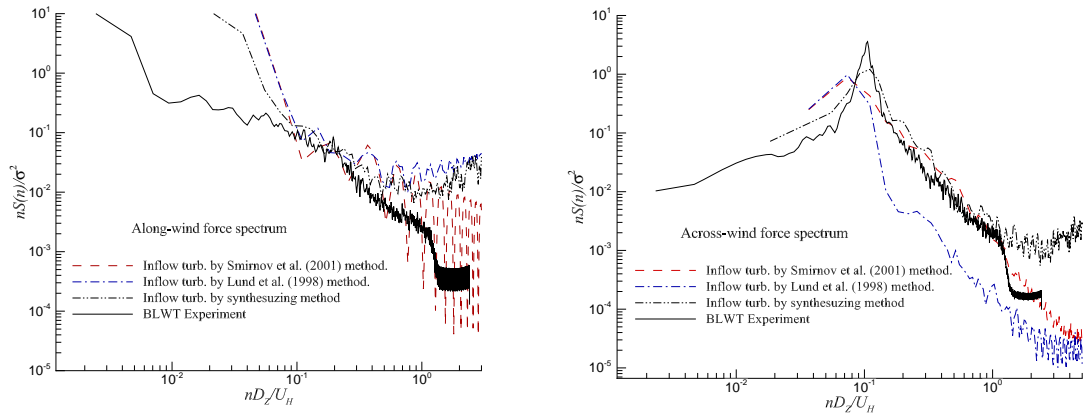


Fig. 19 Along- and across-wind force spectra of a standard tall building using various inflow turbulences

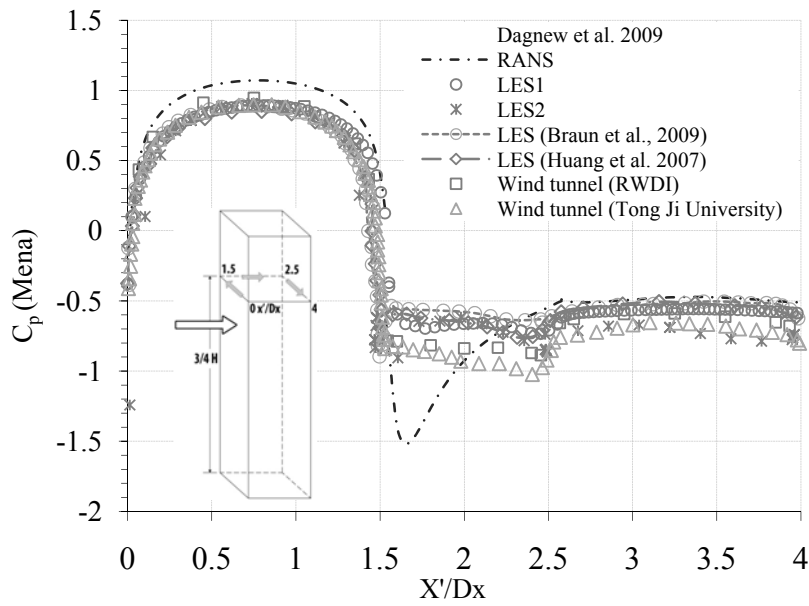


Fig. 20 Mean wind pressure coefficient on CAARC building model. Where the numbers 0 to 4 represent the length of different faces of the CAARC model: from 0 to 1.5: wind-ward, 1.5 to 2.5: side and 2.5 to 4: lee-ward faces

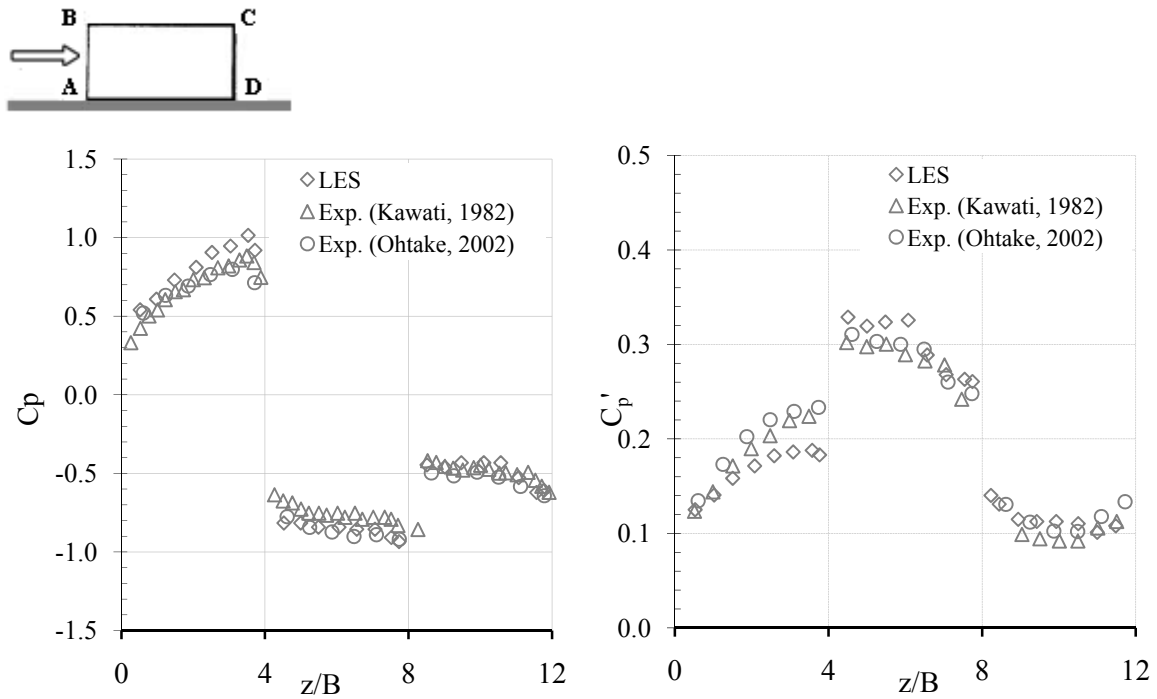


Fig. 21 LES of high-rise building: (a) mean pressure coefficient at a vertical section and (b) rms of pressure coefficient (after Nozawa and Tamura 2002)

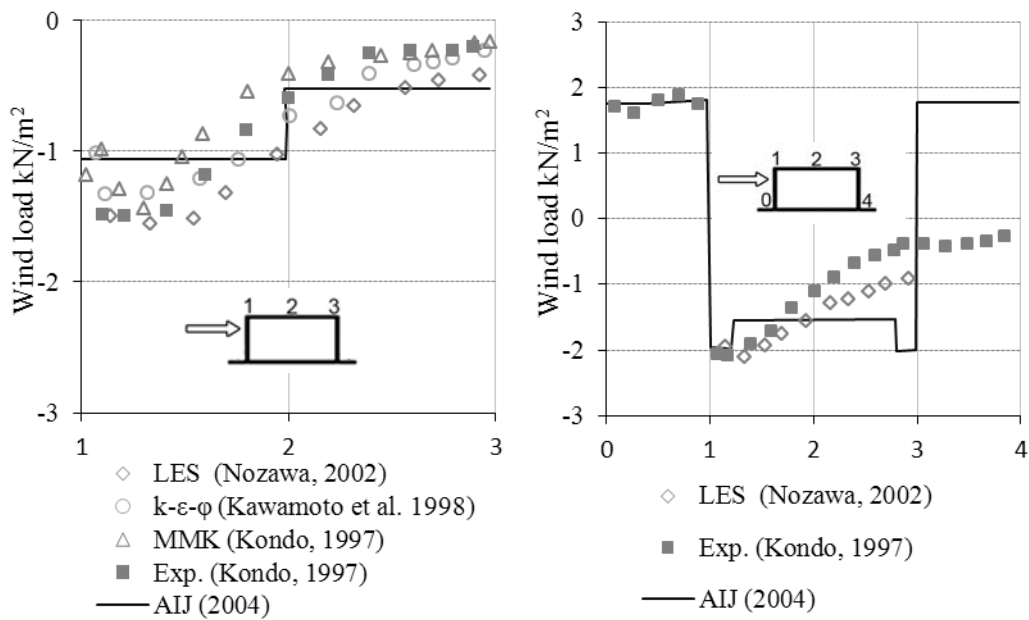


Fig. 22 Comparison of wind loads on low-rise building: (a) structural frame wind load and (b) wind load on cladding (after Tamura *et al.* 2008)

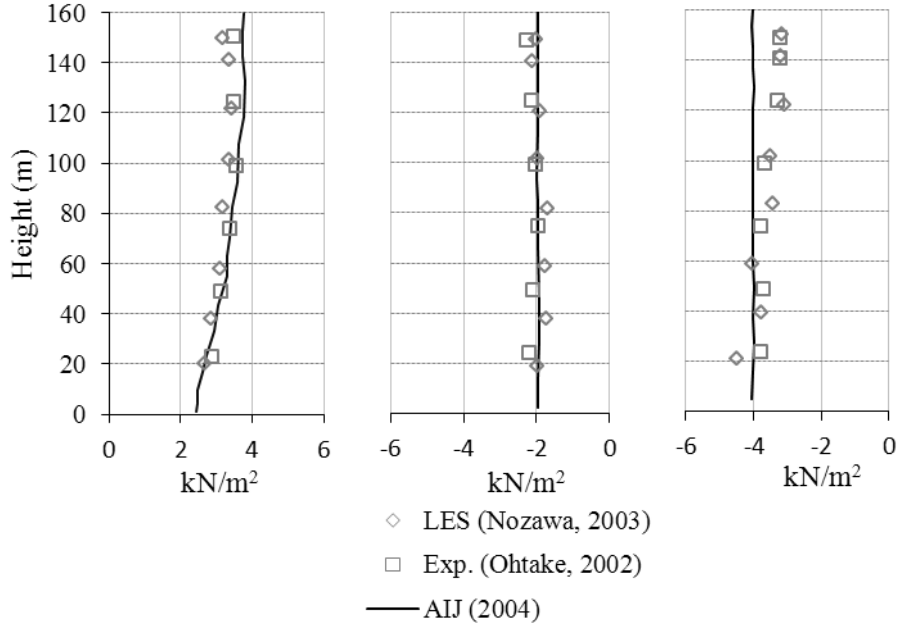


Fig. 23 wind loads on cladding of high-rise building (AIJ, 2005). (a) wind-ward wall, (b) lee-ward wall and (c) side wall (after Tamura *et al.* 2008)

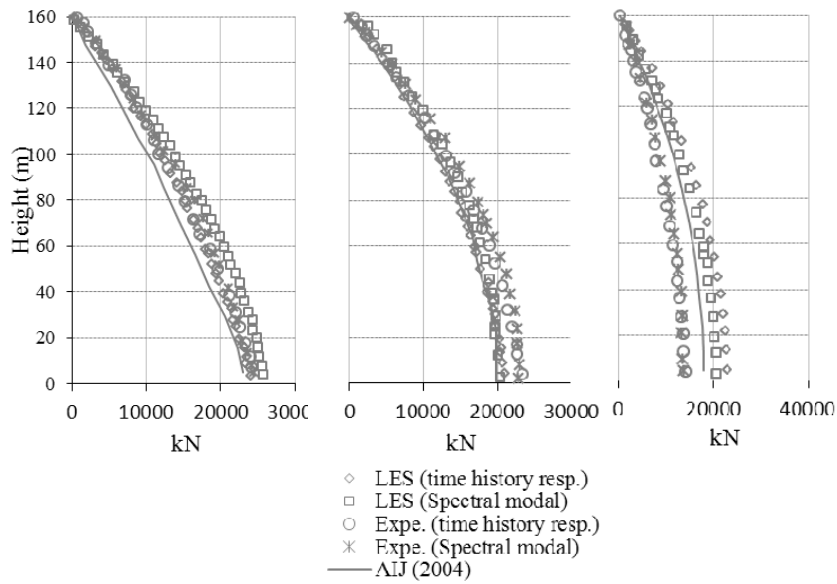


Fig. 24 Wind loads on structural frame of high -rise building: (a) wind-ward, (b) lee-ward and (c) side (after Tamura *et al.* 2008)

Figs. 22(a) and 22(b) show the comparison between numerical and experimental design loading on the structural frame and cladding of a typical short building. The LES overestimated both the structural frame and cladding loading compared to the experimental result. The over-estimation of the wind loads is associated mainly to the insufficient reproduction of the inflow turbulence at the inlet boundary (Tamura, 2008). For the high-rise building (1:1:4) the LES well predicted the design wind loads and coincides well with the experimental results, as shown in Figs. 23 and 24. The transient wind pressure analyses coupled with the realistic inflow turbulence modeling imposed at the inlet boundary were reasons behind the success of the LES results.

7. High performance computing for wind engineering applications

One of the main challenges with CFD applications is the amount of computational resources needed to perform the simulation. The computational cost increases exponentially when attempting to perform large-scale simulations, for example a turbulent wind simulation in a city center requires a very staggering amount of computational resources. This is traditionally handled by using parallel computations on a cluster of central processing units (CPUs) (more recently in combination with graphics processing units (GPUs)). The majority of the available CFD platforms follow this commonly used practice of parallelism. However, the cost of building such a facility could be very expensive. Hence, the application of CWE for realistic simulations of bluff-body aerodynamics with high Reynolds number (Re) numbers flow using advanced turbulence modeling LES has been limited and it still remain more costly than carrying a wind tunnel test. Recently, coupling the general purpose graphics processing units (GPGPUs) that are traditionally designed for graphic rendering purposes with the CPU have been considered as a potential cost-effective alternative of parallel computing for CFD simulations. Implementation of the mixed CPU-GPU techniques have resulted in a substantial speedup of computations (Thibault and Senocak, 2009; Tolke and Krafczyk 2008). Selvam and Landrus (2010) reported that a decent size parallel computing facility with 40 processors configured with the traditional parallel platforms could cost up to \$50,000 while using GPU computing technology which costs \$300 could achieve same efficiency (10 to 20%). And a speed up factor of 10 to 100 could be acquired with a GPU that costs \$100 to \$10,000. Hence, CFD toolboxes that can effectively exploit the hardware of personal computers have economical appeal for the CWE community. This is very encouraging progress towards addressing the computational cost issues involving bluff-body aerodynamics and industrial applications of CWE techniques. Currently there are large number of high performance computing facilities (for example TeraGrid in the US and Sharcnet in Canada) where one can get access for research. Some private firms such as Amazon are also offering the sale of computing time to perform large-scale simulation.

8. Conclusions

The work of several researchers on computational evaluation of wind load both on low- and high-rise buildings have been revisited and key findings on selecting turbulence modeling techniques, boundary conditions, sizing of the computational flow domain, and the dynamics of high Reynolds number turbulent flows have been discussed. The significant progresses made in

turbulence modeling, high performance computing and developments in novel parallel algorithms is allowing a high-resolution simulation of complex flows useful for wind load evaluation. Comparisons made between computationally obtained data with full-scale and model scale wind tunnel experiments showed good agreement, especially on the windward face. However, some discrepancies have been observed in the sidewalls and leeward face. These are mainly attributed to the resolution of the computational meshes and boundary conditions, such as oncoming flow. Numerical inflow turbulence generator that take into account the basic ABL flow statistics (such as TI, wind speed, integral length scale, and the time scale) performed well in reproducing a realistic wind flow field. The along-wind and cross-wind loads on the standard tall building model predicted by the LES simulation showed a good estimation with the experimental data. However, the torsional wind loads obtained by the LES simulation showed some discrepancy with the experiment. Among all the numerical methods considered, LES and hybrid RANS/LES showed a good agreement with the experimental data in most cases. It has also been observed that for wind load estimation an accurate time-dependent analysis using LES, is essential to produce a time-history of pressure fluctuation data, similar to what is being done in wind tunnel experiments. The pressure time-history data obtained from HFPI type LES simulation are very valuable for the estimation of peak-type quantities for the preliminary design of buildings. The peak pressure values are essential wind load parameters in the design of roofs of residential and C&C of tall buildings. Hence enough length of data should be recorded to obtain a good quality of peaks from the LES simulation. However, performing such computationally demanding analyses are limited by current computational resource capabilities and as a result studies on peak pressures are missing from existing literature. It is also to be noted that the cost of performing LES at the moment still appears higher than conducting the BLWT test. Nevertheless, recent developments in the hybrid RANS/LES turbulence modeling show a promising future for CWE practical applications that involve very large projects. The majority of the studies on low- and high- rise buildings have mainly been limited to a single regular shape building for one wind direction. Further research by simulating buildings with more complex shapes, with interference of neighbouring buildings, and for multiple winds including oblique wind directions will accelerate its use as a design tool.

Acknowledgments

This research was supported by the *National Science Foundation CAREER project* under Grant No. 0846811, Any opinions, findings, and conclusions or recommendations expressed in this material are those of the authors and do not necessarily reflect the views of the granting agency.

References

- Nozawa, K. and Tamura, T. (2002), "Large eddy simulation of the flow around a low-rise building immersed in a rough-wall turbulent boundary layer", *J. Wind Eng. And Ind. Aerod.*, **90**, 1151-1162.
- Tamura, T., Nozawa, K. and Kondo, K. (2008), "AIJ guide for numerical prediction of wind loads on buildings", *J. Wind Eng. and Ind. Aerod.*, **96**, 1974-1984.